antibiotics

MDPI

Article

Concomitant effect of quercetin and magnesium doped calcium silicate on osteogenic and antibacterial activity of scaffolds for bone regeneration

A. Preethi [1], and Jayesh R. Bellare [1,2,*]

[1] Department of Chemical Engineering, Indian Institute of Technology Bombay, Mumbai, Maharashtra, India.

[2] Wadhwani Research Center for Bioengineering (WRCB), Indian Institute of Technology Bombay, Mumbai, Maharashtra, India.

* Correspondence: jb@iitb.ac.in

Abstract: Quercetin is a bioflavonoid that has broad spectrum of biological activity. Due to its lower chemical stability, it is usually encapsulated, or a metal-quercetin complex is formed to enhance its biological activity at a lower concentration. Here, our novel approach is to form a quercetin complex to magnesium doped calcium silicate (CMS) ceramics through a coprecipitation technique so as to take advantage of quercetin's antibacterial activity within the antibacterial and osteogenic potential of the silicate. Due to quercetin's inherent metal chelating ability, (Ca+Mg)/Si increased with quercetin concentration. Quercetin in magnesium doped calcium silicate ceramic showed concentration dependent pro-oxidant and antioxidant activity in SaOS-2 with respect to quercetin concentration. By optimizing the relative concentration, we are able to achieve 3x higher proliferation and 1.6x higher total collagen at day 14, 1.7x higher alkaline phosphatase production at day 7 with respect to polycaprolactone/polyvinylpyrrolidone (PCL/PVP) scaffold. Quercetin is effective against Gram positive bacteria like *S. aureus*. Quercetin is coupled with CMS provided similar effect with lower quercetin concentration than quercetin alone. Quercetin reduced bacterial adhesion, proliferation and biofilm formation. Therefore, quercetin coupled magnesium doped calcium silicate not only enhanced osteogenic potential but also reduced bacterial adhesion and proliferation.

Keywords: Quercetin; magnesium doped calcium silicate; osteogenic activity; antibacterial activity; bone regeneration and nanofiber scaffold.

Citation: Preethi, A.; Bellare, J.R.; Synergetic effect of quercetin and magnesium doped calcium silicate on osteogenic and antibacterial activity of scaffolds for bone regeneration. *Antibiotics* **2021**, *10*, x. https://doi.org/10.3390/xxxxx

Academic Editor: Firstname Lastname

Received: date
Accepted: date
Published: date

1. Introduction

Designing resorbable scaffolds for bone tissue engineering is a multifactorial design problem. The current design aspect of scaffold design requires it to reduce/ prevent microbial adhesion and growth and if possible, kill the microbes and also aide in successful bone regeneration. Currently, many of the synthetic polymers like polycaprolactone (PCL) do not possess inherent antibacterial property. Passive resistance against bacteria can be provided by making the scaffold hydrophilic. This can be achieved by including polyvinylpyrrolidone (PVP). Other routes to incorporate antibacterial properties into scaffold can be through the addition of nanoparticle and/or through antibiotics [1]. But the excessive use of antibiotics leads to the development of antibiotic resistant microbes. Therefore, one section of research focuses on identifying biomolecules that can offer properties as that of antibiotics and also supports tissue regeneration.

Quercetin (Q), a phenolic bioflavonoid that is predominantly found in vegetables like onion, has anti-oxidant, anti-inflammatory, anti-bacterial and anti-viral properties [2]. Based on the type of cell type, quercetin can exhibit pro-oxidant or antioxidant effect [3]. Foundational requirement for successful bone regeneration is osteoblastogenesis and angiogenesis. When bone marrow derived mesenchymal stem cells (MSCs) were treated

with 0.1 to 10 μM of Quercetin, MSCs differentiated into osteoblast lineage by upregulating osteoblast specific gene expression. Quercetin inhibits osteoclast by reducing cell proliferation and resorption pits. Also, quercetin enhances angiogenesis by activating vascular endothelial growth factor signaling, upregulating angiogenin-1 [4]. Antibacterial mechanism of flavonoid is different from those of conventional antibiotics. Quercetin exhibits antibacterial activity by decreasing bilayer thickness, opposing bacterial cell-cell signaling, inhibiting biofilm of *E. coli* EAEC 042, inhibiting DNA gyrase and preventing ATP hydrolysis [5]. Viability of *E. coli* and *S. aureus* when treated with 2 μg/ml of quercetin for 24 h was 40% and 60%. This reveals that quercetin did not offer complete bacterial growth inhibition. The efficacy was enhanced by cadmium complexing with N-N bidentate ligands [6].

Even though quercetin has broad spectrum in biological activity, their chemical stability depends on pH, temperature, light and oxidative environment. To enhance the chemical stability, thereby, bioavailability, suitable delivery systems are designed. Their advantages and disadvantages are discussed elsewhere [7]. The sole purpose of many drug delivery system or vehicle is to release the bioflavonoid without affecting its chemical stability. But many of the vehicle mostly does not possess inherent property essential for osteoblast activity. Fabricating bioactive nanoparticle as delivery vehicle for bioflavonoid will enhance the overall biological performance.

Calcium silicate based ceramic nanoparticle demonstrate excellent bioactivity. Their degradation rate can be fine tuned by doping elements like magnesium. This inherently upregulated osteoblast activity. There are various synthesis techniques for magnesium doped calcium silicate (CMS) ceramics [8]. The commonly used techniques like coprecipitation are flexible to accommodate bioflavonoids without compromising its chemical stability. The objective of this article is to investigate the effect of quercetin-CMS system on their ability to enhance osteoblast activity using human osteosarcoma (SaOS-2) cell line and on their ability to resist bacterial adhesion and proliferation.

2. Results

This section discusses about nanoparticle and scaffold characterization under two different subsections.

2.1. Nanoparticle characterization

Magnesium doped calcium silicate (CMS) ceramics prepared through coprecipitation technique rendered them a nano-plate like structure as shown in figure 1. The structure did not change upon quercetin addition. Incorporation of quercetin increased the Mg/Ca ratio in the nanoparticle and also (Ca+Mg)/Si was found to be higher for CMSQ10 nanoparticle (Table 1). FTIR spectra (Figure 2 A) of CMS nanoparticle exhibits Si-O-Si antisymmetric stretching at ~1080 to 1095 cm^{-1} and symmetric stretching at ~465 cm^{-1}. FTIR spectra of quercetin shows C=C stretching in aromatic ring at 1560 cm^{-1} and –OH (phenolic group) at 1379 cm^{-1}. These quercetin functional groups were detected in CMSQ5, CMSQ10 and CMSQ20 nanoparticles, confirming the presence of quercetin in its structure [9]. XRD pattern of all the nanoparticles (Figure 2 B) shows that nanoparticles are amorphous in nature, peaks around 29° shows the characteristic peak of calcium silicate [10]. Peaks of $CaCO_3$ appeared because the nanoparticles were prepared in ambient environment.

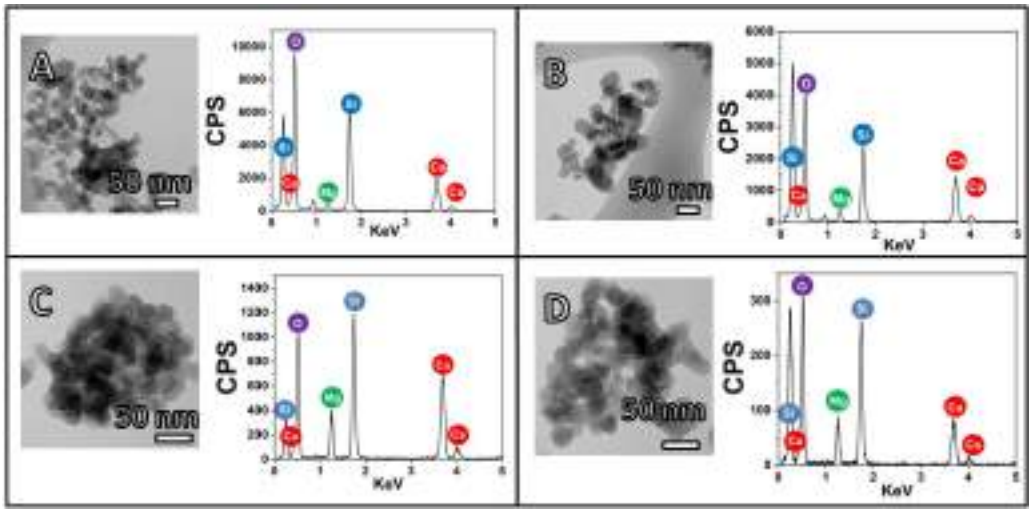

Figure 1. TEM and EDX of A) CMS, B) CMSQ5, C) CMSQ10 and D) CMSQ20 nanoparticles. The shape of all nanoparticle is nano-plate. EDX confirms the presence of calcium, magnesium and silicate ion.

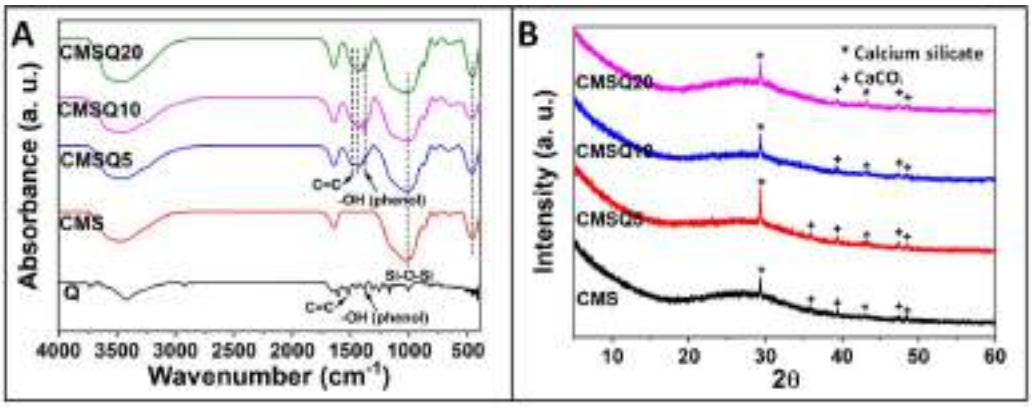

Figure 2. A) FTIR and B) XRD of CMS, CMSQ5, CMSQ10, and CMSQ20 nanoparticles. FTIR confirms the presence of quercetin in its structure. XRD shows the presence of calcium silicate and $CaCO_3$ peaks.

2.2. Scaffold characterization

The scaffold notation PCMSQx (were x= 0, 5, 10 and 20 mg of quercetin per 100 ml of total nanoparticle precursor solution) indicates electrospun scaffold using PCL/PVP as polymer that has quercetin coupled CMS nanoparticle. Electrospinning parameters for the scaffold are tabulated in table 2. Addition of nanoparticle onto polymer solution, altered solution viscosity and conductivity, which in turn required higher flow rate and that affected the nanofiber diameter, nanofiber orientation followed by scaffold surface roughness (figure 3). PCMSQ20 has the least nanofiber diameter that affected the roughness of scaffold (Figure 4 B) Protein adsorption study was done to evaluate the scaffold's ability to attract blood protein upon insertion, thereby it will start the cascade of bone regeneration process. From figure 4 B it is observed that with increasing concentration of quercetin in CMS, protein adsorption reduced. This is due to the hydrophobic nature of quercetin and its strong affinity to BSA protein [25]. With increasing concentration of quercetin in CMS, more quercetin will get released, which will then bind to a hydrophobic BSA protein, preventing it from further adsorption on to the scaffold surface (Figure 4). From ion release study (figure 5) it was revealed that, the amorphous nature of nanoparticles supported ion release. Also, quercetin has interacted with all the ions effectively. With

increase in quercetin concentration, sustained release of silicate ion was observed, because quercetin bounded with silicon.

To study the mechanical property of the scaffold, tensile stress, extension at break and modulus was analysed. It was observed that tensile stress and modulus of the scaffold increased on addition of CMS. Presence of CMS based nanoparticle into the scaffold significantly enhanced the load bearing ability of scaffold by restricting the polymer elongation (figure 6).

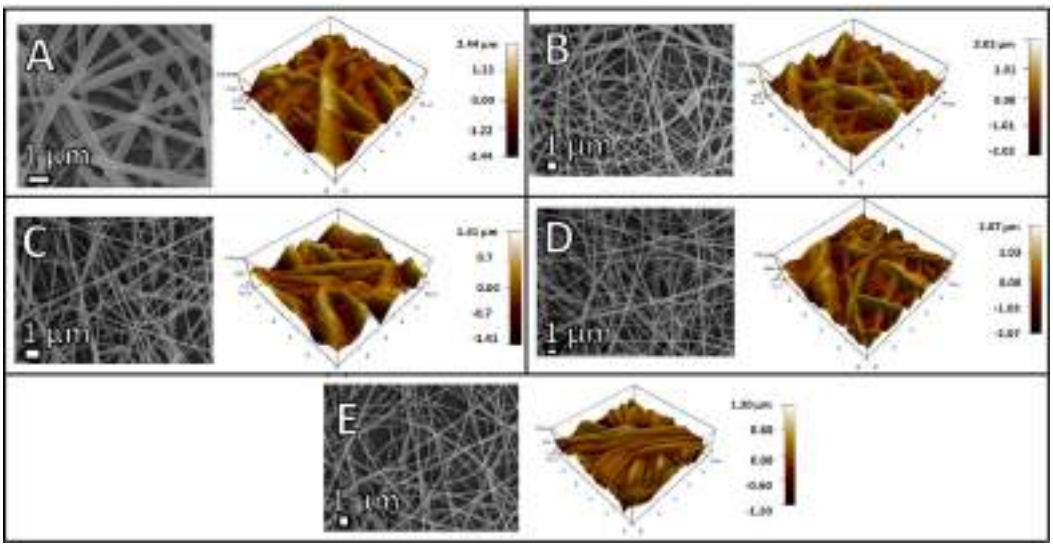

Figure 3. SEM and AFM images of A) P B) PCMS, C) PCMSQ5, D) PCMSQ10 and E) PCMSQ20 scaffolds. Incorporation biomolecule loaded and unloaded CMS nanoparticle has significantly changed the nanofiber diameter and scaffold roughness.

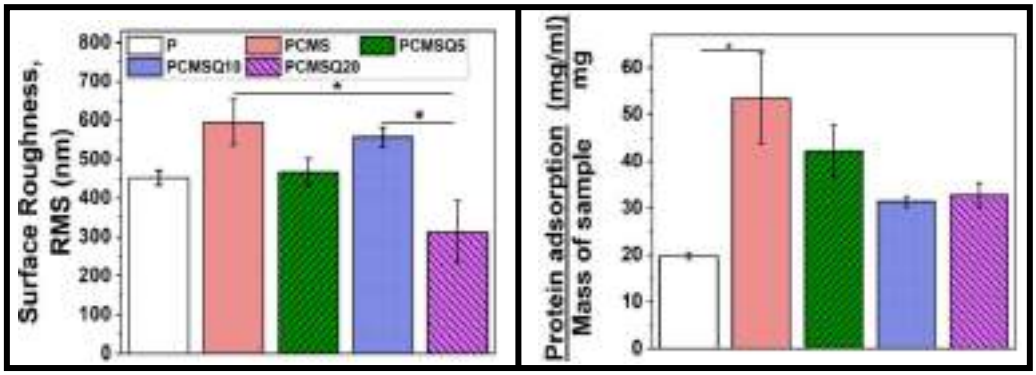

Figure 4. A) Surface roughness and, B) protein adsorption of the scaffold. Nanofiber arrangement altered scaffold roughness. Presence of quercetin affected BSA adsorption.

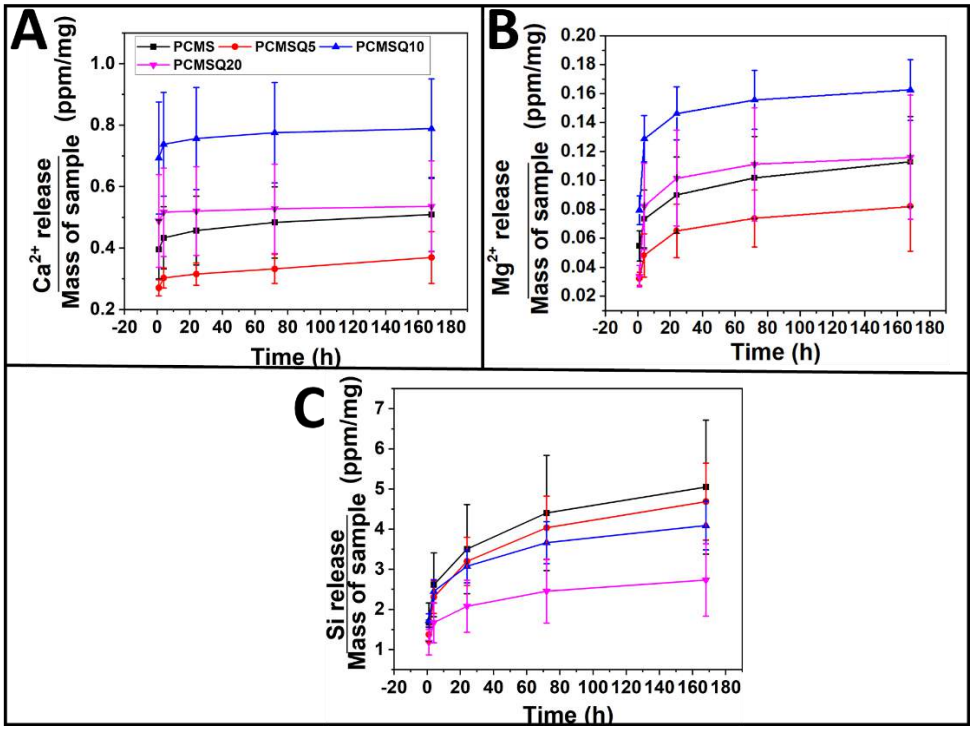

Figure 5. Ion release from the scaffold upon immersion in DI water. A) calcium ion release, B) magnesium ion release and C) silicon ion release from the scaffold. Release of calcium and magnesium ion was similar across all the scaffolds but silicon ion release decreased with increasing quercetin into the nanoparticle.

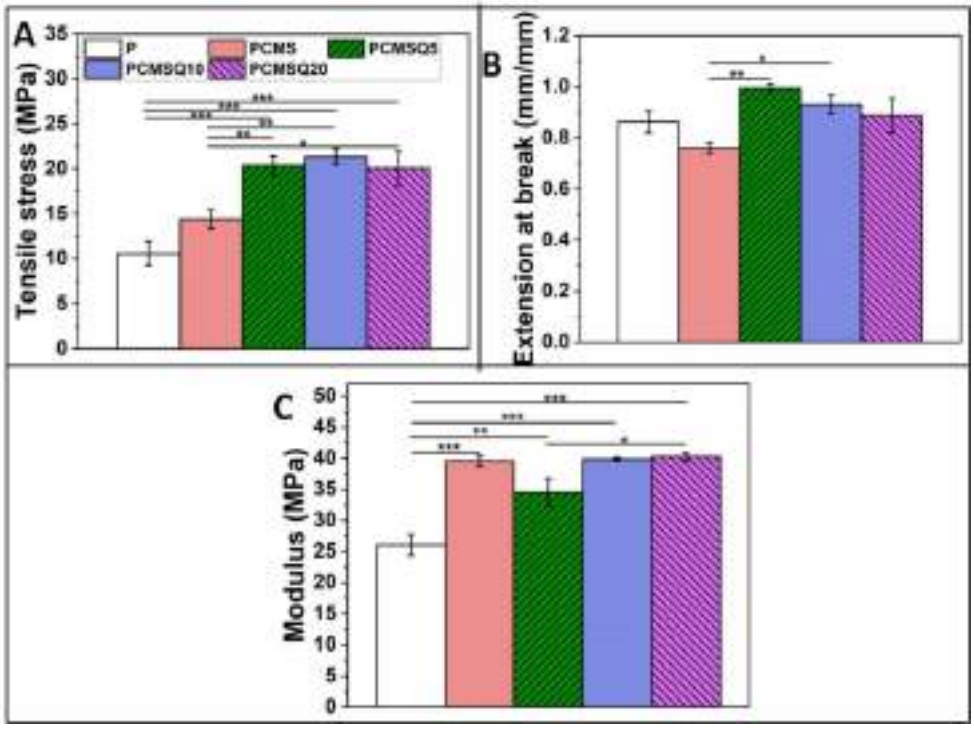

Figure 6. A) Tensile stress, B) extension at break and C) modulus of P, PCMS, PCMSQ5, PCMSQ10 and PCMSQ20 scaffolds. Presence of nanoparticle improved strength of the scaffold, followed by modulus.

The osteogenic potential of the scaffold was tested with MTT assay (Figure 7 A), DNA quantification (Figure 7 B), ALP quantification (Figure 7 C), ROS generation (Figure 7 D) and total collagen synthesis (Figure 7 E) using SaOS-2 cell line. *In-vitro* study of quercetin and CMS system in PCL/PVP scaffold reveals that, presence of quercetin did not affect the osteogenic potential of CMS. The maximum osteogenic potential in the form of higher proliferation, ALP and collagen synthesis was observed for PCMSQ10 scaffold. With further increase in quercetin concentration, intercellular reactive oxygen species (ROS) production was increased which affected the osteogenic potential of the scaffold. The *in-vitro* data is corroborated with confocal images as shown in figure 8.

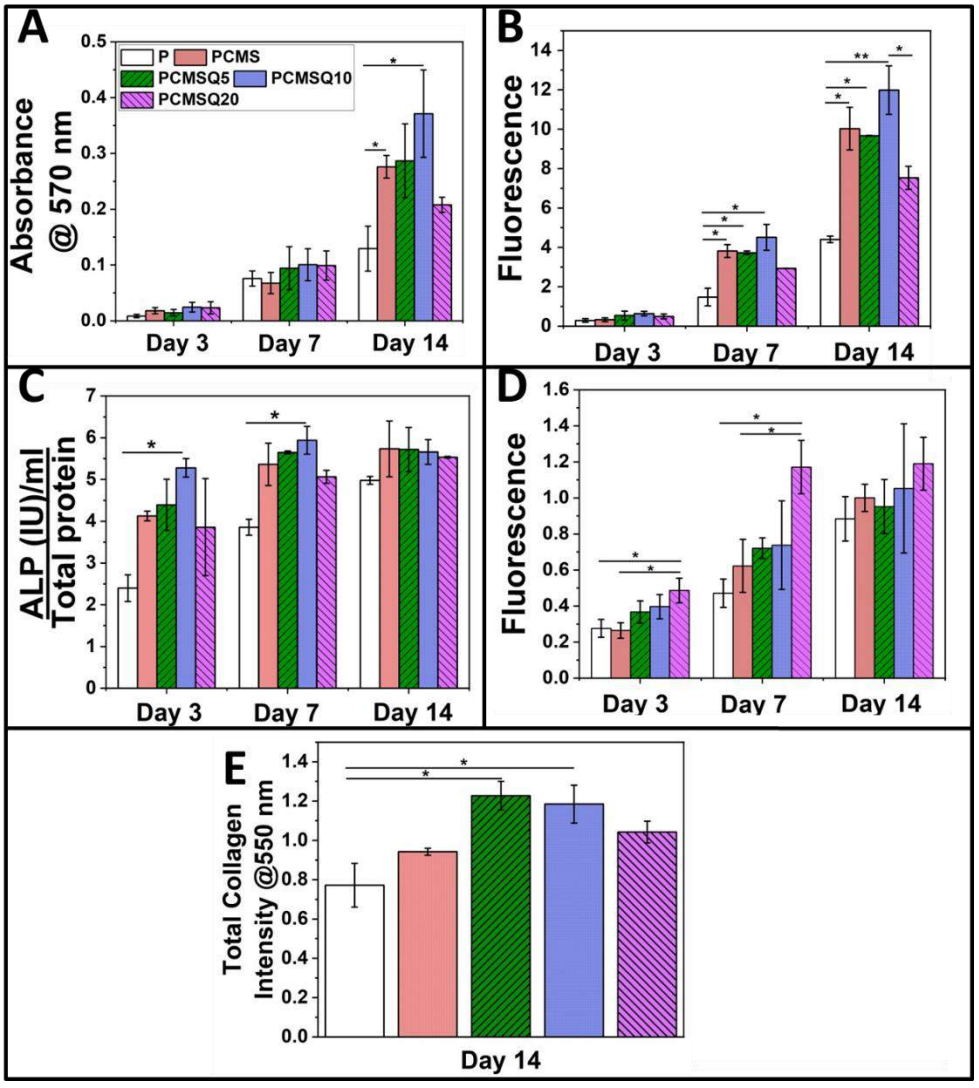

Figure 7. Osteogenic potential assessment (A-E). A) MTT assay, B) DNA quantification, C) ALP (Alkaline phosphatase), D) ROS production, E) total collagen quantification of SaOS-2 and F) quantification of adhered bacteria on scaffold after 12 h on P, PCMS, PCMSQ5, PCMSQ10 and PCMSQ20 scaffolds. Quercetin coupled with CMS increased the osteogenic activity by enhancing osteogenic markers like ALP and collagen production. The maximum acceptable quercetin in the system that can provide osteogenic property is PCMSQ10.

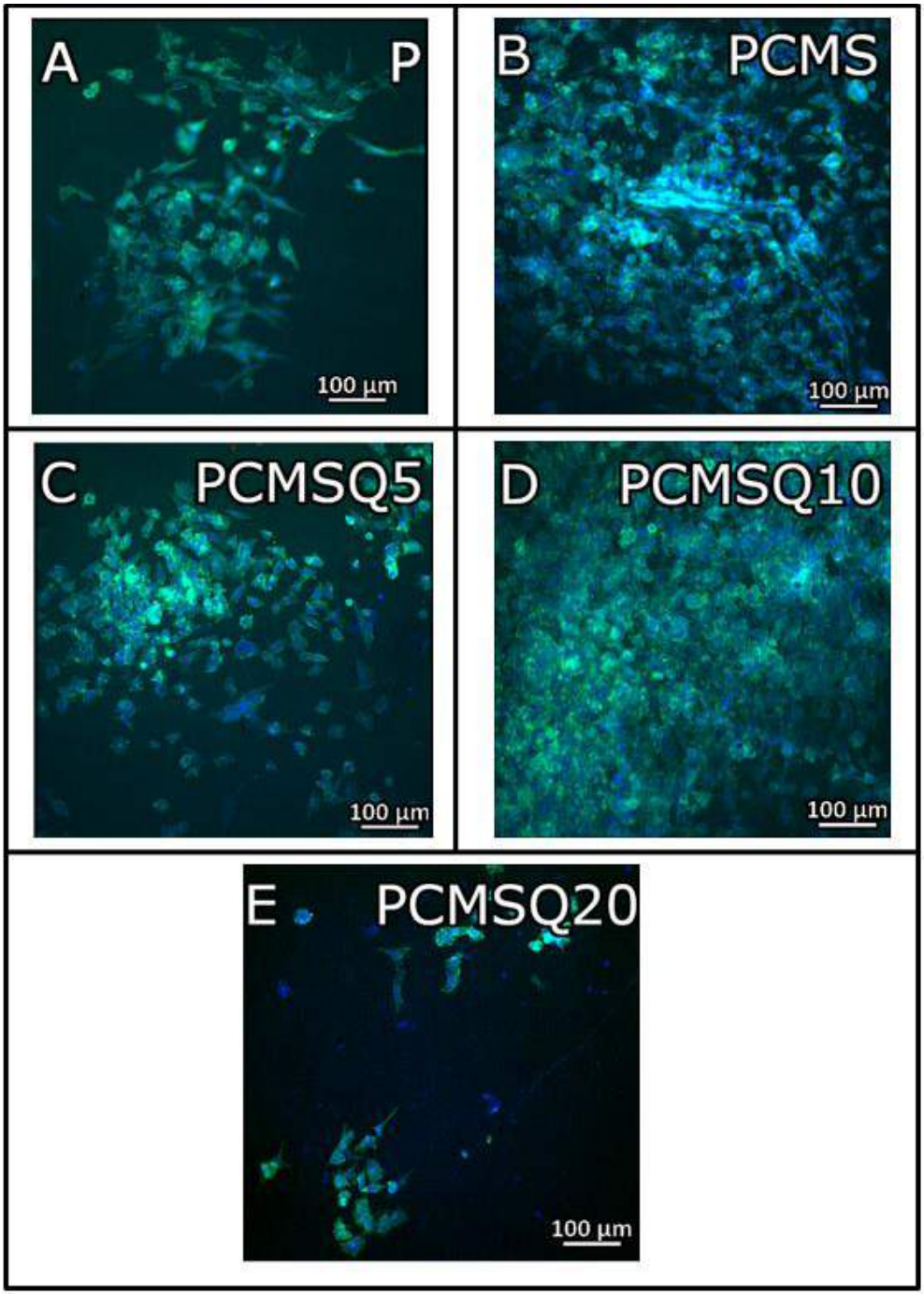

Figure 8. Confocal image of the scaffold at day 14 confirms that, PCMSQ10 has enhanced osteogenic property. The confocal images corroborates with MTT and DNA quantification analysis.

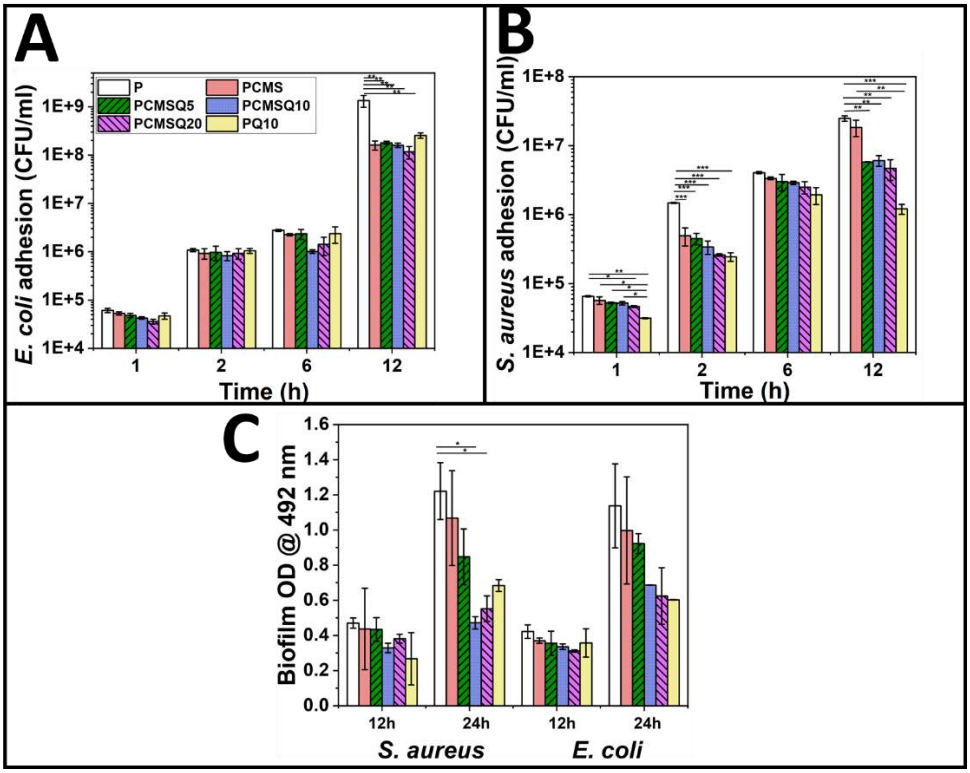

Figure 9. Antibacterial potential assessment of the scaffold. Kinetic study of adhered bacteria A) *E. coli* and B) *S. aureus* on the scaffold. C) Biofilm quantification on the scaffold at 12 h and 24 h. Quercetin is effective against *S. aureus*. Coupling magnesium doped calcium silicate and quercetin reduced *S. aureus* adhesion and biofilm formation at lower quercetin concentration.

The antibacterial activity of the scaffold was analysed by using *E. coli* and *S. aureus*. The scaffold was placed in an environment that supports bacterial proliferation (figure 9). It was observed that, the presence of CMS alone in the scaffold reduced *E. coli* adhesion by 1 log factor. Whereas, for quercetin alone, it requires 10% loading on PCL/PVP (PQ10) to provide similar effect. When quercetin is coupled with CMS, with reduced quercetin loading, bacterial adhesion was reduced by 1 log factor which mainly due to CMS but did not reduce the biofilm formation significantly.

But quercetin is effective against Gram-positive bacteria and reduced the proliferation and biofilm formation in *S. aureus* significantly (Figure 9B). The coupling effect of CMS and quercetin in PCMSQ10 scaffold reduced biofilm formation by 2.4 times compared to scaffold P at 24 h. The SEM of the scaffold with *S. aureus* (figure 10) corroborates the result as shown in figure 9E.

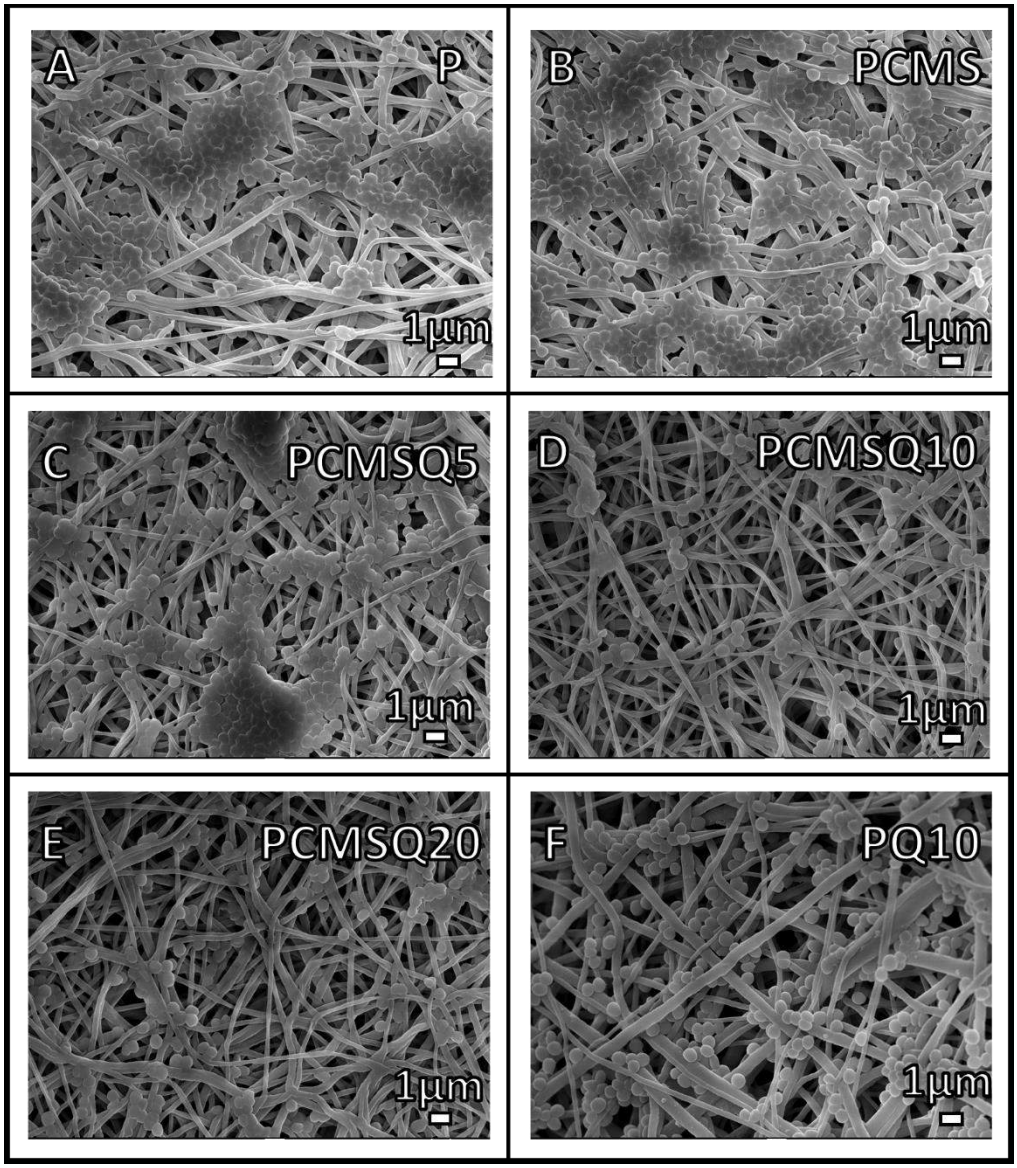

Figure 10. SEM image of *S. aureus* on the scaffolds at 24 h. The scaffold PCMSQ10 has lowest number of adhered bacteria compared to other scaffold. The SEM images correlates well with OD of biofilm.

3. Discussion

Scaffold design for bone tissue regeneration along with local antibiotic therapy is an important research area that aims to avoid post operative infection leading to osteomyelitis. Conventional antibiotic loaded scaffold eliminates microbe at the cost of developing antibiotic resistant bacteria and it also requires additional compounds that imparts osteogenic potential to the scaffold [1]. The research gap can be bridged by finding suitable scaffold system that reduces bacterial adhesion along with improving osteogenic activity.

Synthetic polymer scaffold made out of PCL in general do not possess antibacterial property [1]. They are either blended or modified with a polymer that can provide at least passive resistance to bacterial adhesion. Polymers like polyamides, polyethylene glycol etc., provides antibiofouling effect through passive resistance [1]. PVP is also one such polymer that provides antibiofouling effect, whose incorporation increases hydrophilicity to the scaffold that not only improves osteoblast adhesion but also decreases bacterial adhesion. Their solubility in water provides a suitable platform for enhanced availability of molecules for drug delivery-based scaffold [21].

Flavonoid like quercetin is known to exhibit a spectrum of biological activity. They are synthesized by plant in response to microbial attack. Quercetin has found its foothold in nerve [22], skin tissue engineering applications [23] and also in cancer treatment [24]. Recently, studies on quercetin-based scaffold in bone tissue engineering are gaining attention among researchers because of quercetin's multifaceted property. The dose dependent activity of quercetin is cell line specific. Quercetin at lower concentration supports cell proliferation in nerve [22], skin [23] and bone scaffold but at higher concentration quercetin acts as anticancer agent [24]. Therefore, it is important to give appropriate dosage to bring out the potential of quercetin-based scaffold.

When bone marrow derived MSCs cultured on quercetin inlaid silk hydroxyapatite scaffold revealed that, lowest quercetin concentration i.e., 0.03 wt% has highest ALP production and COL-I and Runx2 gene expression *in-vitro*. *In-vivo* studies on rat calvaria also confirmed that, at 0.03wt%, bone mineral density, bone volume and fraction was found to be higher [11]. When MC3T3-E1 cells were cultured on 3D printed polydopamine-poly (l-lactide) scaffold, it was revealed that, osteogenic activity like cell proliferation, ALP and mineralization was found to be higher for coating concentration up to 200 μM. But the osteogenic activity was lowered for coating concentration of 400 μM [12]. Similarly, when poly (l-lactide) chitosan scaffold coated with polydopamine and 200 μM of quercetin revealed higher cell proliferation, ALP and mineralization by MC3T3-E1 cells [13]. Presence of –OH group in quercetin, helps them chelate with metal ions effectively. Zinc (quercetin)(phenanthroline) complex in PCL/gelatin scaffold enhanced angiogenic and osteogenic activity [14]. Similar effect was found in copper (quercetin)(phenanthroline) complex and copper (quercetin)(neocuproine) complex [15]. From the above metal quercetin complex study it can be understood that, MG-63 cells treated with quercetin concentration above 80 μM shows cytotoxic effect. But the cytotoxic limit got reduced to 60 μM.

Quercetin has better antibacterial activity towards Gram-positive bacteria. Due to their poor water solubility and low chemical stability, they are chemically modified to improve their antibacterial performance [17, 18]. To enhance the quercetin's antibacterial activity, it needs to be complexed with metal ions. Quercetin complexed with Mn^{2+}, Hg^{2+}, Co^{2+} and Cd^{2+} showed antibacterial activity against *S. aureus*, *Bacillus cereus*, *P. aeruginosa*, *E. coli*, and *Klebsiella pneumonia* than quercetin at the similar concentration [5].

So far, to the best of our knowledge, none of the study has focused on dual property (i. e., osteogenic and antibacterial activity) of quercetin in bone tissue engineering. Quercetin expresses both pro-oxidant and antioxidant effect [16]. Therefore, optimizing quercetin concentration that provides the scaffold with dual property has been the aim of this article.

In our study, the osteogenic potential of quercetin showed dose dependent behavior. The coupling CMS and quercetin increased the scaffold's osteogenic activity till PCMSQ10 scaffold i.e., the proliferation and total collagen production was 3x and 1.6x higher than PCL/PVP at day 14. With any further increase in quercetin concentration in the scaffold, scaffold started showing signs of reduced cell viability and osteogenic potential by increasing the ROS production. Similar effect was found in scaffolds used for neural repair [22]. We were able to achieve higher osteogenic potential at lowest quercetin concentration compared to the concentration reported in the literature. This was due to the presence of calcium, magnesium and silicon ions along with quercetin in the scaffold provided favorable outcome in osteoblast activity.

The antibacterial potential of the scaffold was evaluated using *E. coli* and *S. aureus*. CMS quercetin system showed better antibacterial potential towards *S. aureus* from the start of the experiment than *E. coli*. This reveals that Gram positive bacteria are susceptible to quercetin even at the lowest concentration than Gram negative bacteria because quercetin affects *S. aureus*'s cell membrane permeability and integrity [20]. At lower quercetin concentration, antibacterial activity against *E. coli* comes from CMS alone. This may be due to the concentration quercetin inside the scaffold is too low to provide any antibacterial activity against *E. coli*. Our data corroborates with the literature that conveys that the

minimum inhibition concentration of quercetin towards *S. aureus* is much lower than that of *E. coli* [20]. The mode of antibacterial activity in *S. aureus* can be due to outburst of reactive oxygen species and decrease in the proton-motive force in *S. aureus* that affects the membrane permeability [18].

Therefore, our study addressed the important aspect of bridging the anti-microbial research gap by formulating a biomolecule-based scaffold and demonstrating that, it has both osteogenic and antibacterial activity.

4. Experimental

4.1 Materials

Polycaprolactone (PCL, M.W. 80,000 Da), Sodium silicate solution (Extra pure), 3-(4,5-dimethylthiazol-2-yl)-2,5-diphenyltetrazolium bromide (MTT) and Direct Red 80 was purchased from Sigma-Aldrich, India. Polyvinylpyrrolidone (PVP, M.W. 40,000 Da), Magnesium nitrate hexahydrate (98% purity), McCoy's 5A media with ι-glutamine, Fetal Bovine Serum (FBS, Gamma irradiated, sterile filtered, South American) and Antibiotic Antimycotic Solution 100X Liquid (w/10,000 U Penicillin, 10 mg Streptomycin and 25 μg Amphoteric B per ml in 0.9% normal saline) was purchased from Himedia, India. Calcium nitrate tetrahydrate (99% purity) was purchased from S D fine-Chem limited, India. GlutaMAX™-1(100X) was purchased from Thermofisher scientific, India. Picric Acid extrapure AR, 99.8% was purchased from SRL Pvt. Ltd. All chemicals were used as purchased.

4.2 Sample preparation

4.2.1 One pot synthesis of quercetin in calcium magnesium silicate

Solution A containing 0.09 M calcium nitrate tetrahydrate and 0.01 M magnesium nitrate hehahydrate was adjusted to pH 11, before it was mixed with solution B containing 0.1 M sodium silicate. The entire solution was mixed for 30 min. The precipitate was washed and dried overnight. For the quercetin loading, 5, 10, 20 mg of quercetin per 100 ml of total solution was added to solution B and was then mixed with solution A. Nanoparticles with 0, 5, 10, 20 g of quercetin/ml of total solution is named as CMS, CMSQ5, CMSQ10 and CMSQ20. Elemental composition of nanoparticle is given it table 1.

Table 1. Elemental composition of nanoparticle as per TEM.

Sl. No.	Sample code	Elements	(Ca+Mg)/Si	Mg/Ca
1	CMS	Ca, Mg, Si	0.44 ± 0.09	0.28 ± 0.07
2	CMSQ5	Ca, Mg, Si	0.65 ± 0.13	0.28 ± 0.14
3	CMSQ10	Ca, Mg, Si	1.06 ± 0.06	0.48 ± 0.05
4	CMSQ20	Ca, Mg, Si	0.61 ± 0.04	0.69 ± 0.28

4.2.2. Electrospinning solution preparation and nanofiber fabrication

Solution for electrospinning consists of solvent comprises of 2.5 ml dichloromethane and 1 ml methanol and polymer comprises of 0.25 g of PCL and 0.05 g of PVP. The solution is vigorously mixed for 1 h. The nanofiber mat was prepared using 2ml syringe, 23 G blunt needle (BD Discardit™ II syringe, India) in electrospinning machine (ESPIN NANO, India) and is denoted as "P". To prepare nanoparticle incorporated nanofiber mats, 5 wt% of nanoparticles with respect to PCL were added to the above solution and the scaffolds were named as PCMS, PCMS5Q, PCMS10Q and PCMS20Q. All the scaffolds were vacuum dried at room temperature in a desicator and the parameters for electrospinning are given in table 2.

Table 2. Optimised electrospinning parameters of the scaffolds and their fiber diameter.

Sl. No.	Sample code	Flowrate (ml/h)	Voltage (KV)	Distance (cm)	Fiber diameter (nm)
1	P	0.5	25	23	0.56±0.14
2	PCMS	1.2	19	21	0.31±0.07
3	PCMS5Q	1.2	17	17	0.35±0.11
4	PCMS10Q	1.2	19	17	0.24±0.06
5	PCMS20Q	1.2	21	21	0.29±0.06

4.3 Characterization

4.3.1 Scanning electron microscopy (SEM)

Parameters for electrospinning were optimized with the help of field emission gun scanning electron microscopy (JEOL JSM-7600F FEGSEM). All the samples were sputter coated with 10 nm thickness of platinum before analysis.

4.3.2 Transmission electron microscopy (TEM)

Morphology and elemental analysis of the nanoparticles were analysed with the help of JEOL, JEM 2100F and energy dispersive X-ray spectroscopy attached to TEM. To prepare the sample for analysis, few milliGrams of nanoparticles were added to isopropanol and was sonicated for 30 min. Then, few droplets of the above solution were drop casted on top of carbon coated copper grid and dried.

4.3.3 Atomic force microscopy (AFM)

AFM (MFP3D Origin, Asylum/ Oxford Instruments) was to analyse the surface roughness of the scaffold. The scan range is 10*10 μm^2 with a frequency of 0.5/Hz.

4.3.4 Fourier transfer infrared spectroscopy (FTIR)

Nanoparticle's functional groups were analysed with the help of FTIR (3000 Hyperion Microscope with Vertex 80 FTIR system, Bruker, Germany) in the range of 4000-400 cm^{-1}.

4.3.5 X-ray diffraction (XRD)

Phase and crystallinity of nanoparticles were analysed with the help of Rigaku Smartlab X-ray diffractometer with 3 kW X-ray generator Cu tube. The analysis was performed between 2θ of 5^o to 60^o at room temperature with the scan rate of 0.05^o/s.

4.3.6 Ion release study

Scaffold was pre weighed and immersed in 5 ml deionised water at 37 ^oC (DI water). This scaffold was reimmersed into DI water for every time point. The liquid samples were then analysed with the help of Inductively coupled plasma – Atomic emission spectroscopy, ICP-AES (ARCOS, Simultaneous ICP Spectrometer, SPECTRO Analytical Instruments GmbH, Germany).

4.3.7 Quantification of protein adsorption on the scaffold

This analysis was done to understand the effect of quercetin on the scaffolds ability to adsorb bovine serum albumin (BSA). The scaffolds of size of 1 X 1 cm^2 were immersed in 1ml solution containing 5 g/dl of BSA and were incubated for 2 h at 37 ^oC. Next, the

scaffold after incubation was immersed in 1% sodium dodecyl sulfate solution (SDS) for 2 h to strip of adsorbed BSA from the scaffold. Later, the BSA protein in SDS was quantified using Micro BCA Protein Assay Kit 23235 (ThermoFisher scientific, India) as per manufacturer's protocol.

4.3.8 Tensile test

Uniaxial tensile testing of the scaffolds was performed using Instron 2519 series using 5 kN load cell at room temperature with a strain rate of 5 mm/min. Analysis was performed according to ASTM D882 standards.

4.4 *In-vitro* assessment of scaffold using SaOS-2

The human osteosarcoma SaOS-2 cell line was purchased from NCCS, Pune, India and was cultured using McCoy's 5A media containing ι-glutamine containing 1% GlutaMAX™-1(100X), 1% Antibiotic and Antimycotic solution. The cells were maintained in a humidified incubator kept at 37 °C with 5% carbon dioxide (CO_2). For the assays, the scaffolds were placed in non-tissue culture treated 24 well plate (Eppendorf USA), sterilised using 70% ethanol and UV for 1 hr each. The scaffolds were preconditioned using cell culture media for 1 hr each. Cells were seeded at a density of 4 x10^4 cells per cm^2 and incubated for 4 h at 37 °C with 5% CO_2. Afterwards, 0.4 ml media was added in all the wells and was replenished for every 3 days.

Cell viability on the scaffold is evaluated using (3-(4,5-Dimethylthiazol-2-yl)-2,5-Diphenyltetrazolium Bromide) solution (MTT, 1mg/ml in PBS). After culturing cells till a predetermined time point, the scaffolds were washed with PBS and then incubated in 200 µL of MTT solution for 4h followed by adding 800 µL of DMSO to dissolve formazan crystals. The optical density at 470 nm was measured using MultiskanSkyHigh Microplate Spectrophotometer (Thermo-Fischer Scientific, India).

Cell proliferation on the scaffold was assessed using Quant-iT Pico Green DNA assay kit. After culturing cells till a predetermined time point, the scaffolds were washed with PBS and then freeze thawed twice in 500 µL of autoclaved deionized water. The solution was then centrifuged at 10621g for 10 min and then 100 µL of cell lysate supernatant was mixed with 100 µL of Picogreen working solution is mixed and incubated for 5 min as per manufacturer's protocol fluorescence intensity was measured using Varioskan LUX Multimode Microplate Reader at 490/538 nm respectively.

To measure the earlier marker for osteogenic maturation (Alkaline phosphatase), Sensolyte® pNPP Alkaline Phosphatase Assay kit colorimetric was used. The assay was performed as per manufacturer's protocol.

SaOS-2 cells majorly produce collagen type-I, which is also a marker for osteoblast differentiation. To economically quantify total collagen, picosirius red dye is used. To this study, of 1 x10^5 cells were seeded on top of 1.5*1.5 cm^2 scaffold in 12 well plate for 14 days. After culturing cells for 14 days, cells were lysed using 0.2% Triton X-100 prepared in autoclaved deionised water, followed by freeze-thawing and centrifugation (4 °C at 2500 rpm for 10 min). To 100 µL of cell lysate supernatant, 900 µL of Sirius red solution (0.1% direct red dye 80 in saturated picric acid) is mixed for 30 min followed by centrifugation (10 min at 14000 rpm). Supernatant was discarded, then 500 µL of 0.5N NaOH was added to the pellet and then vortexed for 10 min followed by measuring optical density at 550 nm.

Cells on the scaffold was imaged using spinning disc confocal microscopy (Yokogawa Electric Corporation, CSU-X1). Cells in the scaffolds were permeabilized using 0.2% Triton-X 100. Actin filaments were stained using2 units/ml of FITC-phallodin and nucleus is stained using 10 µg/ml of DAPI. Later, images were processed through Zen software (Zeiss).

4.5 *In-vitro* adhesion assessment of *E. coli* and *S. aureus* on scaffold

Micro-organism (*E. coli* K12 or *S. aureus* MTCC 96) at 0.1 optical density (at 600 nm) in LB broth was added to the scaffold and was incubated at 37 °C for 1h, 2h, 6h and 12 h. Later, the scaffold was dipped in 1ml PBS, sonicated for 10 min and vortexed for 1 min to detach the adhered micro-organism from scaffold and was diluted with PBS. After diluting several times, the bacteria was grown on agar plate and the colony forming units per ml was counted. One set of adhered bacteria on the scaffold was dehydrated by serially increasing concentration of ethanol and dried at 37 °C for 12 h and imaged under SEM.

4.6 Biofilm formation on the scaffold

The biofilm formation on the scaffold was quantified by tissue culture plate method [19]. Scaffolds were placed in LB broth for 12h and 24h. Later, the micro-organisms on the scaffolds were fixed using glutaraldehyde (2.5%) at 4 °C for 30 min and dried at 60 °C for 1h. The biofilms were stained using crystal violet (500 µL, 0.1%) solution at room temperature for 20 min followed by rinsing with PBS and dried at 37 °C. Stained biofilm on the scaffold were dissolved in 500 µL of 2% acetic acid for 15 min under gentle agitation. The OD at 492 nm was measured using microplate spectrophotometer.

4 .7 Statistical analysis

Datas represented in this article is the result of at least triplicates of every experiments, expressed as mean ± standard deviation and analyzed using one-way analysis of variance (ANOVA). Significant difference was calculated using tukey's test and are represented as *, ** and *** for $P<0.05$, 0.01 and 0.001.

5. Conclusion

In our study, quercetin coupled CMS nanoparticle were prepared through coprecipitation technique. Quercetin chelated well with ions by increasing (Ca+Mg)/Si ratio. Nanoparticle were incorporated in PCL/PVP matrix and electrospun to produce nanofibrous scaffold. Incorporation of this nanoparticle improved the tensile stress and modulus of the scaffold. The effect of quercetin coupled CMS was optimized to provide improved osteogenic activity by enhancing the proliferation of SaOS-2, ALP and collagen synthesis and inhibiting proliferation of both *E. coli* and *S. aureus* on the scaffold with reduced quercetin loading, making it an attractive material for studies in bone tissue engineering.

Author Contributions

A. Preethi- Conceptualization, methodology, investigation and original draft preparation.

Jayesh R. Bellare- Conceptualization, experimental guidance, review, editing and supervision.

Funding

This research received no external funding.

Acknowledgement

We thank Sophisticated Analytical Instrument Facility, IIT Bombay and Industrial Research and Consultancy Centre, IIT Bombay for providing us with high-end facility for scaffold characterization. We also thank Prof. Rajdip Bandyopadhyaya and Ms. Archana Kumari, Department of Chemical Engineering, IIT Bombay for providing us with MultiskanSkyHigh Microplate Spectrophotometer (Thermo-Fischer Scientific, India) for analysis.

Conflicts of interest

The authors declare no conflict of interest.

References

1. Preethi A, Bellare JR. Tailoring scaffolds for orthopedic application with anti-microbial properties: Current scenario and future prospects. Frontiers in Materials. 2020;7:452. Doi: 10.3389/fmats.2020.594686
2. David AV, Arulmoli R, Parasuraman S. Overviews of biological importance of quercetin: A bioactive flavonoid. Pharmacognosy reviews. 2016 Jul;10(20):84. Doi: 10.4103/0973-7847.194044
3. Kim SY, Jeong HC, Hong SK, Lee MO, Cho SJ, Cha HJ. Quercetin induced ROS production triggers mitochondrial cell death of human embryonic stem cells. Oncotarget. 2017 Sep 12;8(39):64964. doi: 10.18632/oncotarget.11070
4. Wong SK, Chin KY, Ima-Nirwana S. Quercetin as an agent for protecting the bone: A review of the current evidence. International journal of molecular sciences. 2020 Jan;21(17):6448. Doi: 10.3390/ijms21176448
5. Górniak I, Bartoszewski R, Króliczewski J. Comprehensive review of antimicrobial activities of plant flavonoids. Phytochemistry Reviews. 2019 Feb;18(1):241-72. Doi: 10.1007/s11101-018-9591-z
6. Srivastava T, Mishra SK, Tiwari OP, Sonkar AK, Tiwari KN, Kumar P, Dixit J, Kumar J, Singh AK, Verma P, Saini R. Synthesis, characterization, antimicrobial and cytotoxicity evaluation of quaternary cadmium (II)-quercetin complexes with 1, 10-phenanthroline or 2, 2′-bipyridine ligands. Biotechnology & Biotechnological Equipment. 2020 Jan 1;34(1):999-1012. Doi: 10.1080/13102818.2020.1806732
7. Wang W, Sun C, Mao L, Ma P, Liu F, Yang J, Gao Y. The biological activities, chemical stability, metabolism and delivery systems of quercetin: A review. Trends in Food Science & Technology. 2016 Oct 1;56:21-38. Doi: 10.1016/j.tifs.2016.07.004
8. Chen CC, Ho CC, Lin SY, Ding SJ. Green synthesis of calcium silicate bioceramic powders. Ceramics International. 2015 May 1;41(4):5445-53. Doi: 10.1016/j.ceramint.2014.12.112
9. Catauro M, Papale F, Bollino F, Piccolella S, Marciano S, Nocera P, Pacifico S. Silica/quercetin sol–gel hybrids as antioxidant dental implant materials. Science and technology of advanced materials. 2015 May 5. Doi: 10.1088/1468-6996/16/3/035001
10. Wang Y, Zhao Q, Zhou S, Wang S. Effect of C/S Ratio on Microstructure of Calcium Silicate Hydrates Synthesised By Solution Reaction Method. InIOP Conference Series: Materials Science and Engineering 2019 Feb 1 (Vol. 472, No. 1, p. 012003). IOP Publishing. Doi: 10.1088/1757-899X/472/1/012003
11. Song JE, Tripathy N, Lee DH, Park JH, Khang G. Quercetin inlaid silk fibroin/hydroxyapatite scaffold promotes enhanced osteogenesis. ACS applied materials & interfaces. 2018 Sep 6;10(39):32955-64. Doi: 10.1021/acsami.8b08119
12. Chen S, Zhu L, Wen W, Lu L, Zhou C, Luo B. Fabrication and evaluation of 3D printed poly (L-lactide) scaffold functionalized with quercetin-polydopamine for bone tissue engineering. ACS Biomaterials Science & Engineering. 2019 Apr 25;5(5):2506-18. Doi: 10.1021/acsbiomaterials.9b00254
13. Zhu L, Chen S, Liu K, Wen W, Lu L, Ding S, Zhou C, Luo B. 3D poly (L-lactide)/chitosan micro/nano fibrous scaffolds functionalized with quercetin-polydopamine for enhanced osteogenic and anti-inflammatory activities. Chemical Engineering Journal. 2020 Jul 1;391:123524. Doi: 10.1016/j.cej.2019.123524
14. Preeth DR, Saravanan S, Shairam M, Selvakumar N, Raja IS, Dhanasekaran A, Vimalraj S, Rajalakshmi S. Bioactive Zinc (II) complex incorporated PCL/gelatin electrospun nanofiber enhanced bone tissue regeneration. European Journal of Pharmaceutical Sciences. 2021 May 1;160:105768. Doi: 10.1016/j.ejps.2021.105768
15. Vimalraj S, Rajalakshmi S, Preeth DR, Kumar SV, Deepak T, Gopinath V, Murugan K, Chatterjee S. Mixed-ligand copper (II) complex of quercetin regulate osteogenesis and angiogenesis. Materials Science and Engineering: C. 2018 Feb 1;83:187-94. Doi: 10.1016/j.msec.2017.09.005
16. Kim SY, Jeong HC, Hong SK, Lee MO, Cho SJ, Cha HJ. Quercetin induced ROS production triggers mitochondrial cell death of human embryonic stem cells. Oncotarget. 2017 Sep 12;8(39):64964. Doi: 10.18632/oncotarget.11070
17. Kho W, Kim MK, Jung M, Chong YP, Kim YS, Park KH, Chong Y. Strain-specific anti-biofilm and antibiotic-potentiating activity of 3′, 4′-difluoroquercetin. Scientific Reports. 2020 Aug 25;10(1):1-9. Doi: 10.1038/s41598-020-71025-7
18. Osonga FJ, Akgul A, Miller RM, Eshun GB, Yazgan I, Akgul A, Sadik OA. Antimicrobial activity of a new class of phosphorylated and modified flavonoids. ACS omega. 2019 Jul 30;4(7):12865-71. Doi: 10.1021/acsomega.9b00077

19. Ma R, Lai YX, Li L, Tan HL, Wang JL, Li Y, Tang TT, Qin L. Bacterial inhibition potential of 3D rapid-prototyped magnesium-based porous composite scaffolds–an in vitro efficacy study. Scientific reports. 2015 Sep 8;5(1):1-4. Doi: 10.1038/srep13775
20. Wang S, Yao J, Zhou B, Yang J, Chaudry MT, Wang M, Xiao F, Li Y, Yin W. Bacteriostatic effect of quercetin as an antibiotic alternative in vivo and its antibacterial mechanism in vitro. Journal of Food Protection. 2018 Jan;81(1):68-78. Doi: 10.4315/0362-028X.JFP-17-214
21. Kurakula M, Koteswara Rao GS. Moving polyvinyl pyrrolidone electrospun nanofibers and bioprinted scaffolds toward multidisciplinary biomedical applications. European Polymer Journal. 2020 Aug 1;136:109919. Doi: 10.1016/j.eurpolymj.2020.109919
22. Jang SR, Kim JI, Park CH, Kim CS. The controlled design of electrospun PCL/silk/quercetin fibrous tubular scaffold using a modified wound coil collector and L-shaped ground design for neural repair. Materials Science and Engineering: C. 2020 Jun 1;111:110776. Doi: 10.1016/j.msec.2020.110776
23. Ajmal G, Bonde GV, Mittal P, Khan G, Pandey VK, Bakade BV, Mishra B. Biomimetic PCL-gelatin based nanofibers loaded with ciprofloxacin hydrochloride and quercetin: A potential antibacterial and anti-oxidant dressing material for accelerated healing of a full thickness wound. International journal of pharmaceutics. 2019 Aug 15;567:118480. Doi: 10.1016/j.ijpharm.2019.118480
24. Zhang H, Zhang M, Yu L, Zhao Y, He N, Yang X. Antitumor activities of quercetin and quercetin-5′, 8-disulfonate in human colon and breast cancer cell lines. Food and Chemical Toxicology. 2012 May 1;50(5):1589-99. Doi: 10.1016/j.fct.2012.01.025
25. Papadopoulou A, Green RJ, Frazier RA. Interaction of flavonoids with bovine serum albumin: a fluorescence quenching study. Journal of agricultural and food chemistry. 2005 Jan 12;53(1):158-63. Doi: 10.1021/jf048693g